arXiv:0906.5590v1 [gr-qc] 30 Jun 2009

On Wormholes supported by phantom energy

J. A. González,[1] F. S. Guzmán,[1] N. Montelongo-García,[1] and T. Zannias[1]

[1]*Instituto de Física y Matemáticas, Universidad Michoacana de San Nicolás de Hidalgo. Edificio C-3, Cd. Universitaria, A. P. 2-82, 58040 Morelia, Michoacán, México.*

(Dated: June 30, 2009)

By a combination of analytical and numerical techniques, we demonstrate the existence of spherical, asymptotically flat traversable wormholes supported by exotic matter whose stress tensor relative to the orthonormal frame of Killing observers takes the form of a perfect fluid possessing anisotropic pressures and subject to linear equations of state: $\tau = \lambda\rho c^2$, $P = \mu\rho c^2$. We show that there exists a four parameter family of asymptotically flat spherical wormholes parametrized by the area of the throat $A(0)$, the gradient $\Lambda(0)$ of the red shift factor evaluated at the throat as well as the values of (λ,μ). The latter are subject to restrictions: $\lambda > 1$ and $2\mu > \lambda$ or $\lambda < 0$ and $2\mu < -|\lambda|$. For particular values of (λ,μ), the stress tensor may be interpreted as representing a phantom configuration, while for other values represents exotic matter. All solutions have the property that the two asymptotically flat ends posses finite ADM mass.

PACS numbers: 04.20.-q, 04.25.D-, 04.40.-b

I. INTRODUCTION

The observed late time accelerated expansion of the universe [1, 2] appears to imply that the universe is dominated by dark energy [3], a substance having the property that if $(\rho c^2, P)$ stand for the energy density and isotropic pressure as measured by observes co-moving with the expansion, then P is negative or more precisely $\rho c^2 + 3P < 0$. This property is often stated that the equation of state (EOS) for dark energy is $w = \frac{P}{\rho c^2} < -\frac{1}{3}$. Additional observations of CMB, gravitational lensing and supernovae [4], mildly favor a more exotic EOS: $w = \frac{P}{\rho c^2} < -1$ and such substance is dubbed as phantom energy. The possibility that the cosmic fluid is in state of phantom energy has another consequence. The stress tensor describing phantom energy violates the null energy condition and thus phantom energy is the type matter required to support wormholes [5].

The issue whether a static spherical distribution of phantom energy can support spherical wormholes has been addressed in [6, 7]. In these works phantom energy is modeled by a perfect fluid stress tensor possessing anisotropic pressures with the radial pressure $P_r = -\tau$ and energy density ρc^2 obeying: $w = \frac{P_r}{\rho c^2} = -\frac{\tau}{\rho c^2} < -1$ while the tangential pressure P is defined by the field equations. In [6] an a-priori choice for the energy density has been made whereas in [7] the wormhole metric has been a priori specified.

In the present work, we model exotic matter by a stress tensor so that relative to orthonormal frame of Killing observers takes the form of a perfect fluid possessing anisotropic pressures but we assume that ρc^2, τ and P are subject to constraints referred as the EOS. Guided by the cosmological phantom EOS and generality purposes we adopt [8]:

$$\tau = \lambda\rho c^2, \quad P = \mu\rho c^2, \quad \lambda,\mu \in I\!R, \tag{1}$$

where (λ,μ) are treated as free parameters subject only to the restriction that the stress tensor should violate the null energy condition in an open vicinity of the throat and restrictions arising by demanding asymptotic flatness. The problem of the existence of spherical wormholes supported by this type of exotic matter, is formulated as an initial value problem (IVP here after) with the throat serving as initial value surface (for more details regarding this approach see [9], [10]). By a combination of analytical and numerical techniques we show that there exist initial conditions and values of (λ,μ) where solutions of this IVP describe asymptotically flat non singular wormholes. Asymptotic flatness requires (λ,μ) to obey either $\lambda > 1$ and $2\mu > \lambda$ or $\lambda < 0$ and $2\mu < -|\lambda|$. Thus even though (λ,μ) play a secondary role in the behavior of the solutions near the throat, they determine the asymptotic behavior of the solution.

The structure of the present paper is as follows: In the following section we formulate the relevant IVP and discuss some properties of this IVP while in sections III we discuss numerical solutions. In section IV we present an analysis that explains the numerical outputs and advance arguments that set restrictions upon (λ,μ) so that the solutions describe asymptotically flat wormholes. We finish the paper with a discussion concerning the results and future work.

II. LOCAL WORMHOLES SUPPORTED BY A "PERFECT FLUID"

We consider a static, spherically symmetric wormhole:

$$\mathbf{g} = -e^{2\Phi(l)}dt^2 + dl^2 + r^2(l)d\Omega^2, \quad l \in (-\alpha, \alpha), \quad \alpha > 0, \tag{2}$$

where $r(l=0) \neq 0$, $\frac{dr(l)}{dl}|_0 = 0$, $\frac{d^2r(l)}{dl^2}|_0 > 0$ and thus $l = 0$ marks the location of the throat. We support this wormhole with a stress tensor $T_{\alpha\beta}$ so that relative to the orthonormal frame of Killing observers decomposes according to:

$$\begin{aligned} T_{\alpha\beta} &= \rho(l)c^2 u_\alpha u_\beta - \tau(l) X_\alpha X_\beta + P(l)(Y_\alpha Y_\beta + Z_\alpha Z_\beta), \\ \mathbf{u} &= e^{-\Phi(l)}\frac{\partial}{\partial t}, X = \frac{\partial}{\partial l}, \ Y = \frac{1}{r(l)}\frac{\partial}{\partial \theta}, \ \ Z = \frac{1}{r(l)\sin\theta}\frac{\partial}{\partial \phi}. \end{aligned} \tag{3}$$

In the gauge of (2), if we define $\hat{r}(l) = r^{-1}(l)$, introduce $K(l) = \frac{2}{r(l)}\frac{dr(l)}{dl}$ the trace of the extrinsic curvature of the $SO(3)$ orbits as embedded in t =cons hyper-surfaces and $\Lambda(l) = \frac{d\Phi(l)}{dl}$, then $G_{\alpha\beta} = \hat{k}T_{\alpha\beta}$ taking into account (1) can be cast in the form [9, 10]:

$$\frac{d\hat{r}(l)}{dl} = -\frac{1}{2}K(l)\hat{r}(l), \tag{4}$$

$$\frac{dK(l)}{dl} = -\frac{3}{4}K^2(l) + \hat{r}^2(l) - \hat{k}\rho(l)c^2, \tag{5}$$

$$\frac{d\Lambda(l)}{dl} = -K(l)\Lambda(l) - \Lambda^2(l) + (1 - \lambda + 2\mu)\frac{\hat{k}\rho(l)c^2}{2}, \tag{6}$$

$$\frac{d\rho(l)}{dl} = \rho(l)\left[(\frac{1}{\lambda} - 1)\Lambda(l) - (1 + \frac{\mu}{\lambda})K(l)\right], \tag{7}$$

$$-\hat{r}^2(l) + \frac{K^2(l)}{4} + \hat{k}\rho(l)c^2\lambda + \Lambda(l)K(l) = 0. \tag{8}$$

A throat of area $A(0) = 4\pi r^2(0)$ requires tension $\tau(0)$ so that $\hat{k}\tau(0) = r^{-2}(0)$ and moreover: $(\tau(0) - \rho(0)c^2) > 0$ [11]. These conditions in view of (1) take the form:

$$\hat{k}\lambda c^2\rho(0) = r^{-2}(0), \quad [\tau(0) - \rho(0)c^2] = (\lambda - 1)\rho(0)c^2 > 0, \tag{9}$$

and thus they hold, provided either $(\rho(0) > 0, \lambda > 1)$ or $(\rho(0) < 0, \lambda < 0)$. If we adopt as a definition that an inhomogeneous phantom configuration satisfies $w = \frac{P_r}{\rho c^2} = -\frac{\tau}{\rho c^2} < -1$, then the first choice yields: $w = -\lambda < -1$ and thus $T_{\alpha\beta}$ describes a phantom like configuration at least in an open vicinity of the throat. For the second choice, even though $\rho(0) < 0$ nevertheless $\tau(0)$ is positive and for this case we interpret $T_{\alpha\beta}$ as describing exotic matter [12].

Any solution of (4-8) describes a local wormhole having a throat of area $A(0) = 4\pi r^2(0) = 4\pi\hat{r}^{-2}(0)$ at a prescribed $\Lambda(0)$, provided it satisfies the initial conditions [11]:

$$\hat{r}(0) = \left(\frac{4\pi}{A(0)}\right)^{1/2}, \quad K(0) = 0, \quad \Lambda(0), \quad \rho(0) = \frac{4\pi}{\lambda\hat{k}c^2 A(0)}. \tag{10}$$

The system (4-7) combined with these initial conditions constitutes a well defined IVP. The theorem of "Picard-Lindelof" [13] assures the local existence of a unique C^1 solution defined on $[-b, b] \subset (-\alpha, \alpha)$. Ideally, we would like to find necessary or (and) sufficient conditions so that these local solutions are extendible for all $l \in (-\infty, \infty)$ and moreover represent asymptotically flat wormholes. Due to the non linearities in (4-7) this is a formidable task. In this work we shall gain insights into the properties of the maximal solutions by first resorting to numerical techniques. It is our hope that these insights will eventually contribute towards an analytical treatment of the problem.

For the purpose of numerical integrations, we compactify the coordinate l via:

$$l(x) = \frac{r_0 x}{1 - x^2}, \quad x \in (-1, 1), \quad r_0 = r(0). \tag{11}$$

This transformation maps $l \to \pm\infty$ into $x \to \pm 1$, $l = 0$ into $x = 0$ and transforms (4-7) into:

$$
\begin{aligned}
(1-x^2)^2 \frac{d\hat{r}(x)}{dx} &= -\frac{r_0}{2}(1+x^2)K(x)\hat{r}(x), && (12)\\
(1-x^2)^2 \frac{dK(x)}{dx} &= r_0(1+x^2)\left[-\frac{3}{4}K^2(x) + \hat{r}^2(x) - \hat{k}\rho(x)c^2\right], && (13)\\
(1-x^2)^2 \frac{d\Lambda(x)}{dx} &= r_0(1+x^2)\left[-K(x)\Lambda(x) - \Lambda^2(x) + \frac{\hat{k}\rho(x)c^2}{2}(1-\lambda+2\mu)\right], && (14)\\
(1-x^2)^2 \frac{d\rho(x)c^2}{dx} &= r_0(1+x^2)\left[\left(\frac{1}{\lambda}-1\right)\Lambda(x) - \left(1+\frac{\mu}{\lambda}\right)K(x)\right]\rho(x)c^2, && (15)
\end{aligned}
$$

and leaves the initial conditions (10) form invariant. We integrate the IVP defined by these equations combined with (10) for a variety of initial conditions and values of (λ, μ). Before we enter into numerics, we mention three properties of smooth solutions of this IVP.

- Any C^1 solution $(\hat{r}(x), K(x), \Lambda(x), \rho(x))$ generated by initial conditions so that $\Lambda(0) = 0$, is “reflectionally symmetric” relative to the throat i.e. under “ parity” transformation $x \to -x$ behaves according to [14]:

$$r(x) = r(-x),\ \ K(x) = -K(-x),\ \ \Lambda(x) = -\Lambda(-x),\ \ \rho(x) = \rho(-x). \tag{16}$$

- If $(\hat{r}(x), K(x), \Lambda(x), \rho(x))$ is any C^1 solution generated by an arbitrary set of initial conditions, then the functions:

$$R(x) = \hat{r}(-x),\ \ K_1(x) = -K(-x), L(x) = -\Lambda(-x),\ \ \hat{\rho}(x) = \rho(-x), \tag{17}$$

  define a new solution that satisfies the same initial conditions as $(\hat{r}(x), K(x), \Lambda(x), \rho(x))$ does, except that $L(0) = -\Lambda(0)$.

- If $(\hat{r}(x), K(x), \Lambda(x), \rho(x))$ is any solution, then under rescaling of the throat

$$\hat{r}(0) \to \hat{r}^{'}(0) = A\hat{r}(0), \quad A > 0, \tag{18}$$

  it follows that

$$A\hat{r}(x), \quad AK(x), \quad A\Lambda(x), \quad A^2\rho(x), \tag{19}$$

  satisfy (12-15) and the rescaled initial conditions (10).

Property (16) implies that for reflectionally symmetric solutions, integrating (12-15) on the domain $(0, 1)$ would be sufficient. Property (17) allows us to concentrate on solutions obeying $\Lambda(0) \geq 0$ while (19) permits us to set the throat radius at some convenient value.

III. NUMERICAL RESULTS

We integrate (12-15) subject to (10), using a Runge-Kutta integrator of different accuracy and in order to avoid the singularity at $x = \pm 1$, we stagger the exact points $x = \pm 1$. In all runs we employ units so that $c = G = 1$ and thus $\hat{k} = 8\pi$. We set the throat radius $r(0) = 1$ and employ the following two sets of initial conditions [11]:

$$
\begin{aligned}
&\hat{r}(0) = 1,\ \ K(0) = 0,\ \ \Lambda(0),\ \ \rho(0) = \frac{1}{8\pi\lambda},\ \ \lambda > 1, && (20)\\
&\hat{r}(0) = 1,\ \ K(0) = 0,\ \ \Lambda(0),\ \ \rho(0) = \frac{1}{8\pi\lambda},\ \ \lambda < 0. && (21)
\end{aligned}
$$

At first we consider reflectionally symmetric solutions i.e. set $\Lambda(0) = 0$ and choose $\lambda = 1.5$ and $\mu \in \{1, 0.5, -0.5\}$. The resulting solution curves are shown in Fig. 1. In a second run we maintain $\Lambda(0) = 0$ but choose $(\lambda = -0.5, \mu = 0.5)$, $(\lambda = -1, \mu = -0.25)$ and $(\lambda = -1, \mu = 0.5)$ and the graphs are shown in Fig. 2.

A number of runs aims to get insights in the behavior of reflectionally symmetric solutions upon changing the value of $\Lambda(0)$. For these runs we consider a reflectionally symmetric solution for fixed (λ, μ), and vary $\Lambda(0)$ from $\Lambda(0) = 0$ towards positive and negative values. We have used three different values for (λ, μ) and the results of these runs are shown in Figs. 3,4,5.

Case	λ	μ	Behavior
1	1.5	1	Asym. Flat
2	1.5	0.5	Decaying Non - Asym.Flat
3	1.5	-0.5	Non - Asym.Flat
4	-0.5	0.5	Non - Asym.Flat
5	-1	-0.25	Decaying Non - Asym.Flat
6	-1	-0.5	Asym.Flat

TABLE I: Table showing the values of the parameters (λ, μ) used in Figs. 1,2.

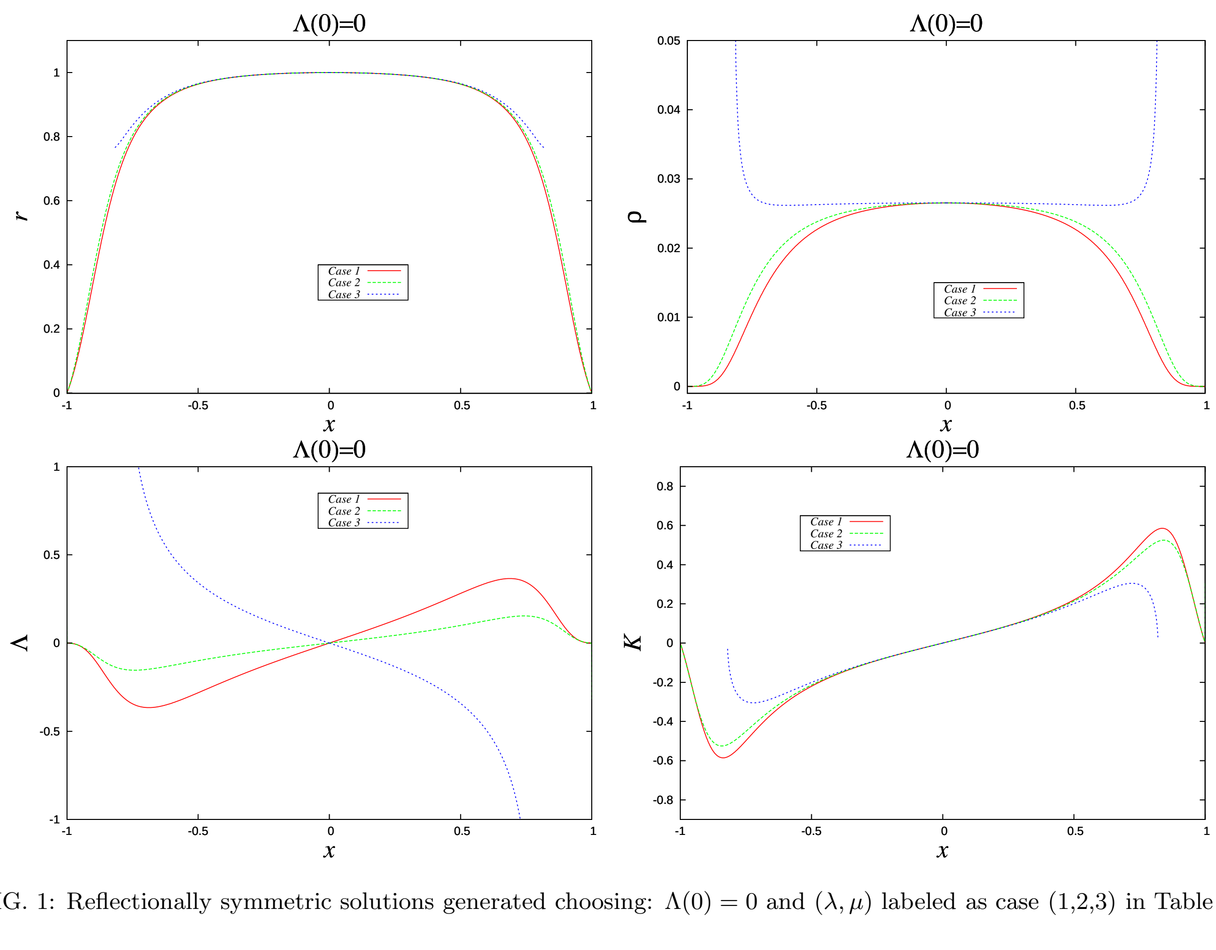

FIG. 1: Reflectionally symmetric solutions generated choosing: $\Lambda(0) = 0$ and (λ, μ) labeled as case (1,2,3) in Table I.)

IV. EXISTENCE OF ASYMPTOTICALLY FLAT WORMHOLES

The numerical outputs displayed in Figs. 1-5 show that solutions are divided into two families: the first one contains solutions where all variables decay to zero as $x \to \pm\, 1$ whereas the second one contains solutions where the variables become unbounded in one (or both) ends. This behavior raises a number of questions: Which if any, of the decaying

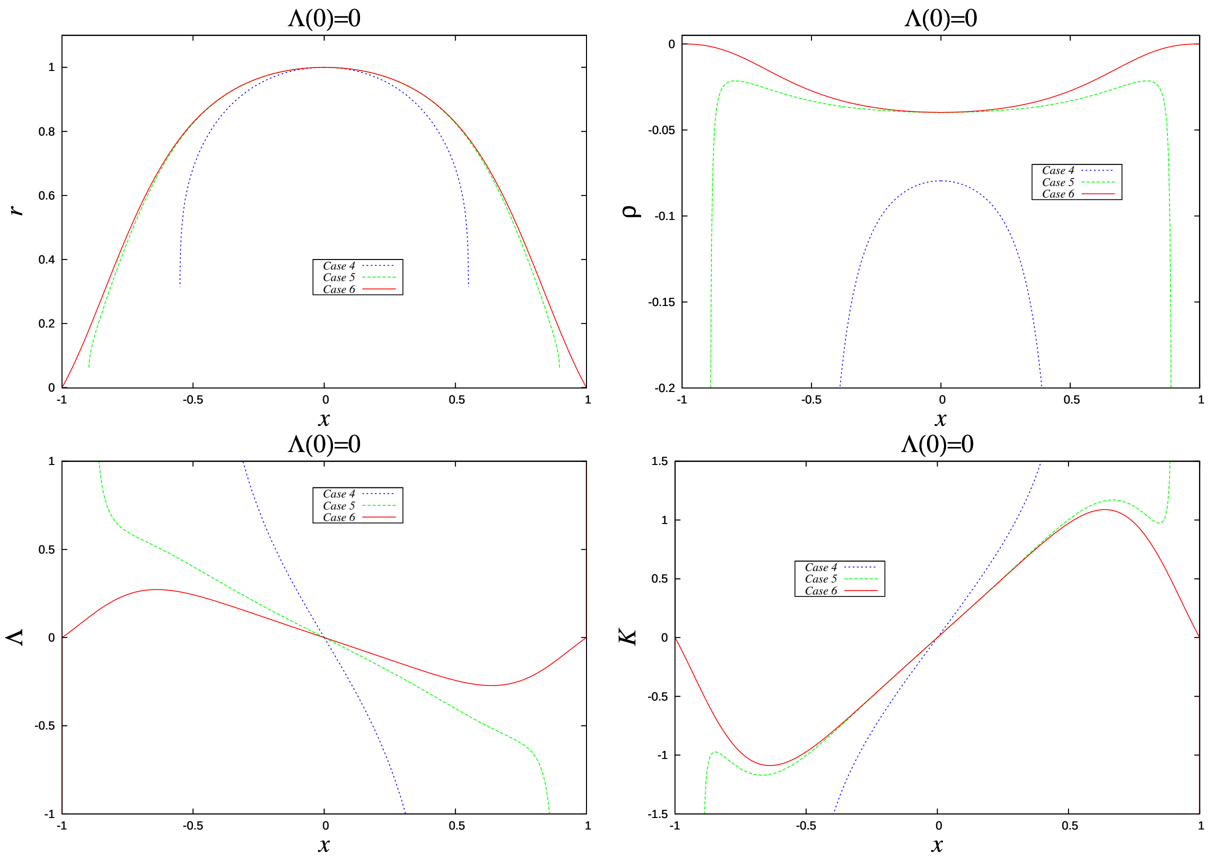

FIG. 2: Reflectionally symmetric solutions generated by choosing: $\Lambda(0)=0$, and (λ,μ) labeled as case (4,5,6) in Table.)

to zero solutions describe asymptotically flat wormholes? How the initial conditions and values of (λ,μ) affect the global behavior of the solutions? Bellow, we provide an explanation of that behavior and draw a few conclusions based on these graphs.

We begin by first discussing an exact solution of (4-8). This solutions is generated by choosing (λ,μ) so that $1-\lambda+2\mu=0$ and taking $\Lambda(l)=0$ as the global solution of eq. (6). The restriction $1-\lambda+2\mu=0$ implies that the EOS takes the form:

$$\tau=\lambda\rho c^2,\ P=\frac{\lambda-1}{2}\rho c^2,\ \lambda>1 \text{ or } \lambda<0. \tag{22}$$

and the resulting solution in curvature coordinates is described by (for details see [15]):

$$\mathbf{g} \ = \ -dt^2+\frac{dr^2}{1-\left(\frac{r_0}{r}\right)^{\frac{\lambda-1}{\lambda}}}+r^2d\Omega^2,\ r \ \in \ (r_0,\infty), \tag{23}$$

$$\hat{k}\rho(r)c^2 \ = \ \frac{1}{r_0^2\lambda}\left(\frac{r_0}{r}\right)^{\frac{3\lambda-1}{\lambda}},\ r \ \in \ (r_0,\infty). \tag{24}$$

For latter use, we notice that for $\lambda>1$, the density decays according to $\hat{k}\rho(r)c^2=O(r^{-(2+\epsilon)}),\ 0<\epsilon<1$, while for $\lambda<0$, $\hat{k}\rho c^2=O(r^{-(3+\epsilon)}),\ \epsilon>0$.

In the remaining part of this section we analyze the asymptotic behavior of the solutions. We consider a solution that decays to zero as $l\to\pm\infty$ (the graphs in Figs. 1-5 show that such solutions exist). For such solution and away from the throat we introduce coordinates (t,r,θ,ϕ) so that:

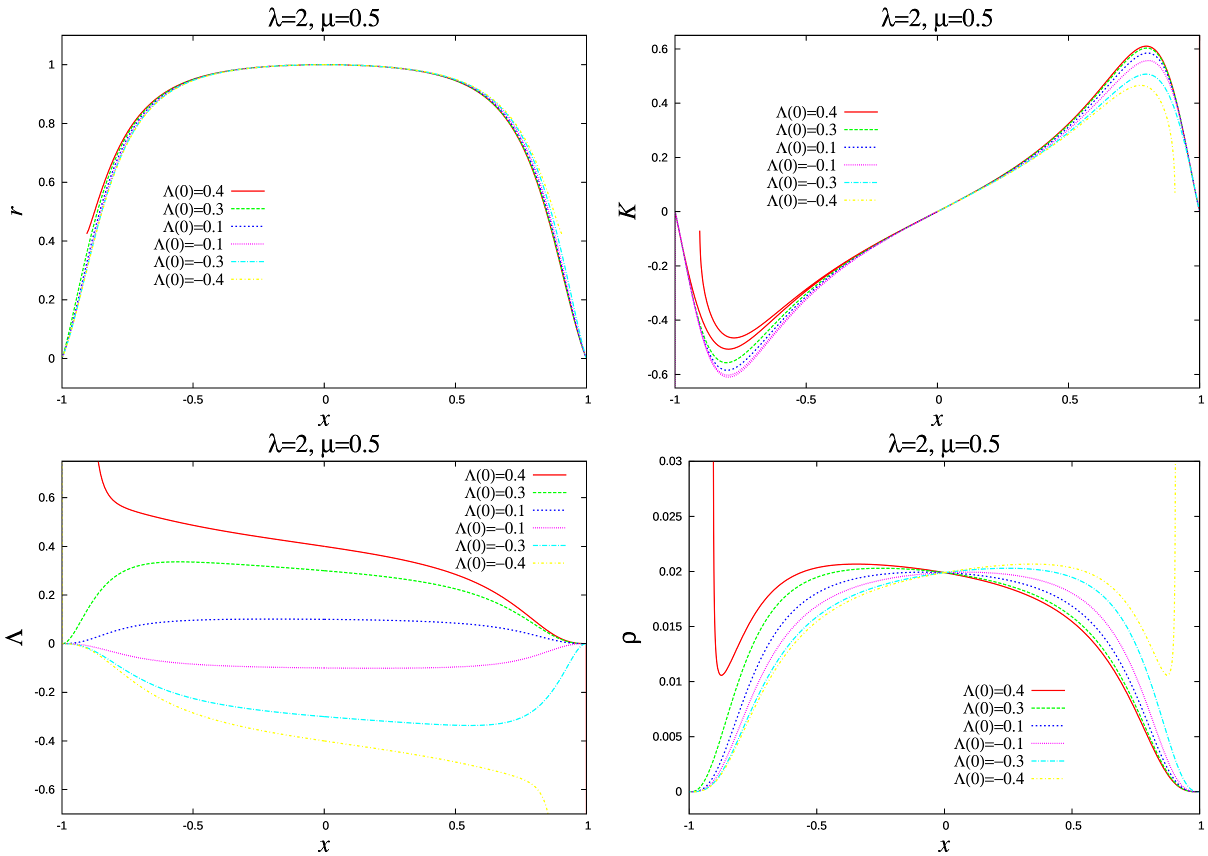

FIG. 3: In these graphs we have taken $\lambda = 2$, $\mu = 0.5$ so that $1 - \lambda + 2\mu = 0$, and we have kept them constants throughout. We gradually change $\Lambda(0)$ starting from $\Lambda(0) = 0$ and increasing (decreasing) towards positive (negative) values. Notice that after a characteristic value of $\Lambda(0)$ the solutions become unbounded at one end.

$$\mathbf{g} \;=\; -e^{2\Phi(r)}dt^2 + \frac{dr^2}{1 - \frac{2m(r)}{r}} + r^2 d\Omega^2, \quad r > r_0 = r(0) > 0, \tag{25}$$

$$m(r) \;=\; \frac{r_0}{2} + \frac{\hat{k}c^2}{2}\int_{r_0}^{r} r'^{\,2}\rho(r')dr'. \tag{26}$$

Either from (4-7) or directly from $G_{\alpha\beta} = \hat{k}T_{\alpha\beta}$ we find:

$$\frac{dm(r)}{dr} = \frac{\hat{k}c^2}{2}r^2\hat{\rho}(r), \quad r \;\in\; (r_0, \infty), \tag{27}$$

$$\frac{d\tau(r)}{dr} = \left[\rho(r)c^2 - \tau(r)\right]\frac{d\Phi(r)}{dr} - \frac{2[P(r) + \tau(r)]}{r}, \quad r \;\in\; (r_0, \infty), \tag{28}$$

$$\frac{d\Phi(r)}{dr} = \frac{-\hat{k}\tau(r)r^3 + 2m(r)}{2r(r - 2m(r))}, \quad r \;\in\; (r_0, \infty). \tag{29}$$

Taking into account the EOS and introducing the variables:

$$W(r) = \frac{2m(r)}{r}, \quad R(r) = \hat{k}\rho(r)c^2r^2, \tag{30}$$

(27-29) become:

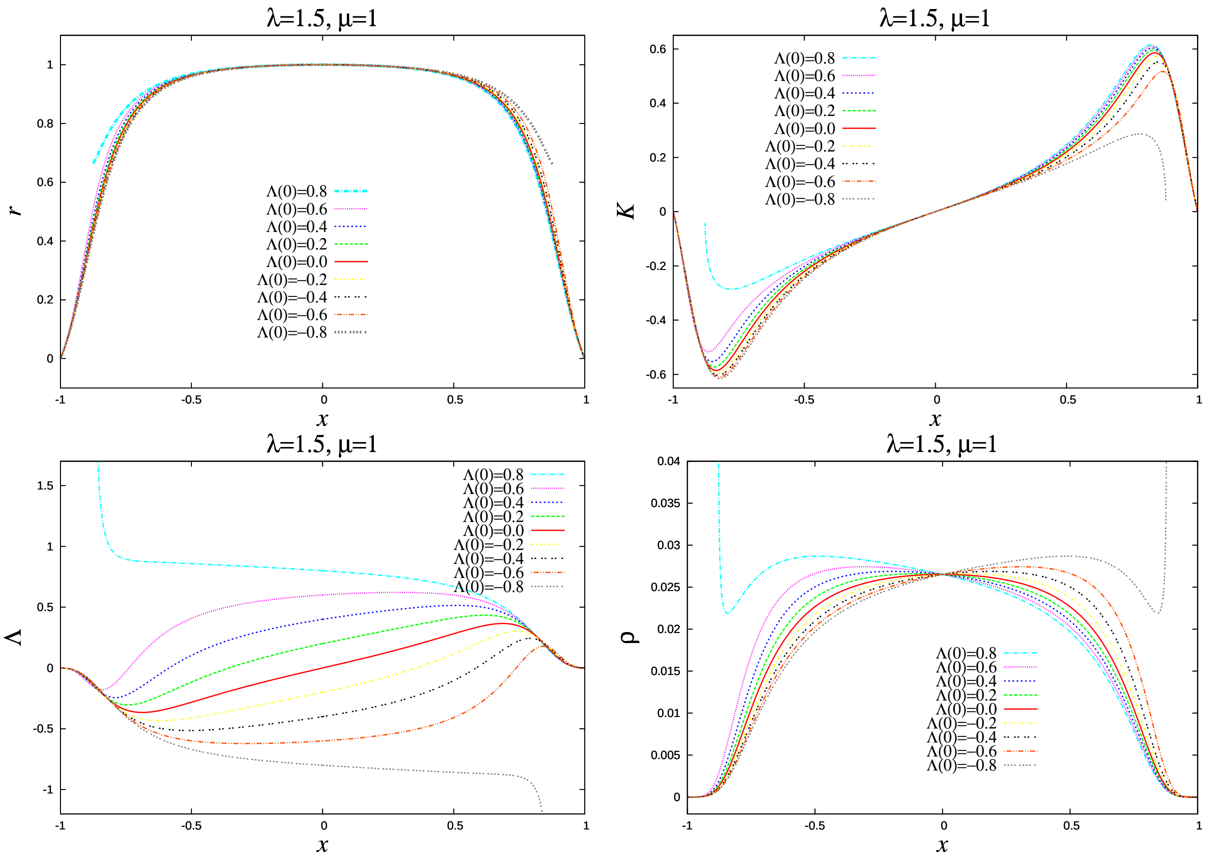

FIG. 4: In the graphs we have taken $\lambda = 1.5$, $\mu = 1$. Like in Fig.(3), we vary $\Lambda(0)$ from $\Lambda(0) = 0$ up to $\Lambda(0) = 0.8$ and $\Lambda(0) = -0.8$. Again after some characteristic value of $\Lambda(0)$ the solutions become diverging at one end.

$$r\frac{dW(r)}{dr} = -W(r) + R(r), \tag{31}$$

$$r\frac{dR(r)}{dr} = -\frac{2\mu}{\lambda}R(r) + \left(\frac{1}{\lambda} - 1\right)\frac{-\lambda R(r) + W(r)}{2(1 - W(r))}R(r), \tag{32}$$

$$r\frac{d\Phi(r)}{dr} = \frac{-\lambda R(r) + W(r)}{2(1 - W(r))}. \tag{33}$$

This system becomes singular at three places: as $r \to r_0$, on any $r \in (r_0, \infty)$ so that $W(r) = 1$, and as $r \to \infty$. Since for our background solution all fields decay to zero as $l \to \pm\infty$, we assume that (31-33) is defined in a domain $[R_0, \infty)$ where R_0 is sufficiently large so that:

$$W(r) < 1,\ \ R(r) < 1\ ,\forall \quad r \ \in \ [R_0, \infty). \tag{34}$$

and additionally: $\lim_{r\to\infty} W(r) = 0$, $\lim_{r\to\infty} R(r) = 0$. On $[R_0, \infty)$ we introduce a new variable t via:

$$r = r_0 e^t, t \ \in \ [T, \infty), \quad T = \log\left(\frac{R_0}{r_0}\right), \tag{35}$$

so that (31-33) becomes an autonomous system:

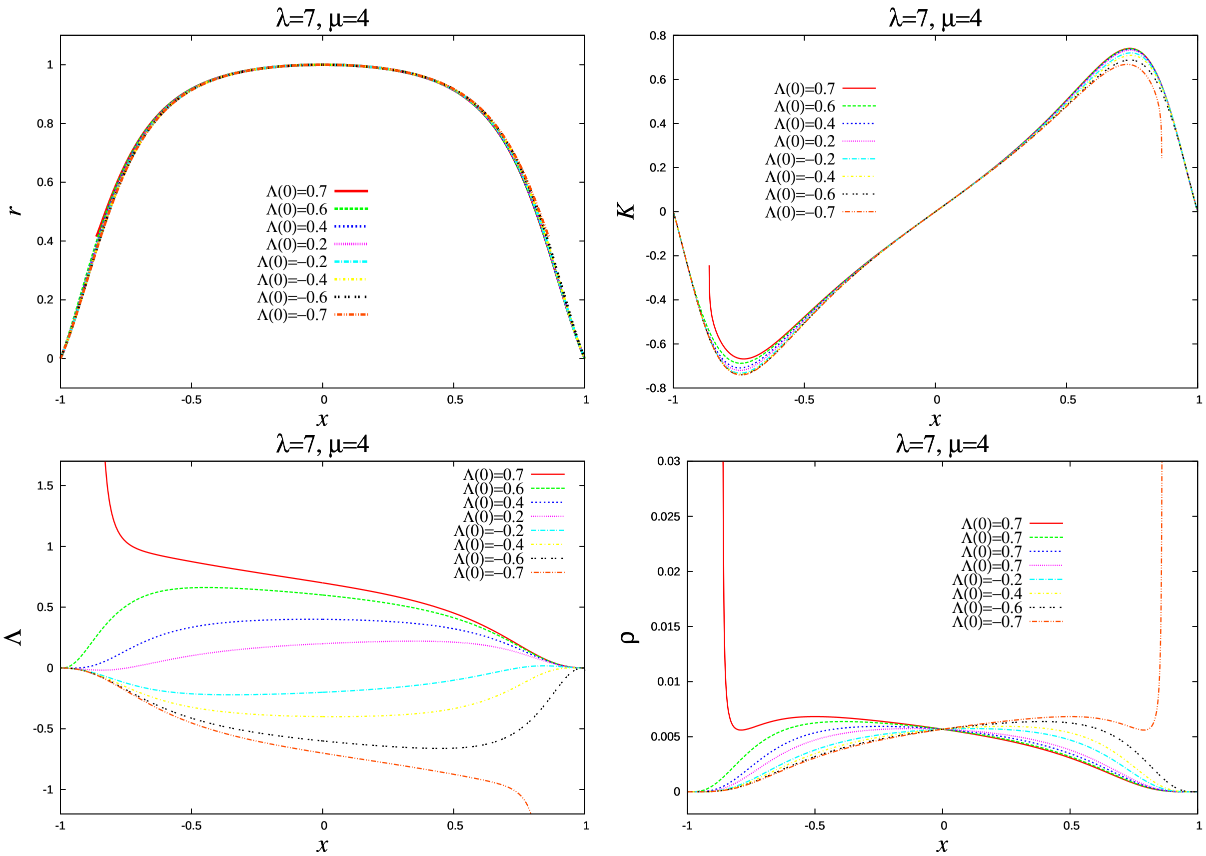

FIG. 5: We repeat the same analysis as in Figs. (3, 4) except that we have chosen $\lambda = 7,\ \mu = 4$. Again, the solutions diverge after some characteristic value of $\Lambda(0)$.

$$\frac{dW(t)}{dt} = -W(t) + R(t), \tag{36}$$

$$\frac{dR(t)}{dt} = -\frac{2\mu}{\lambda}R(t) + \left(\frac{1}{\lambda} - 1\right)\frac{-\lambda R(t) + W(t)}{2(1 - W(t))}R(t), \tag{37}$$

$$\frac{d\Phi(t)}{dt} = \frac{-\lambda R(t) + W(t)}{2(1 - W(t))}. \tag{38}$$

Since solutions of (38) are determined by $(W(t), R(t))$, we restrict our attention to the first two equations. They can be written in the form:

$$\frac{d\mathbf{x}(t)}{dt} = \Lambda\mathbf{x}(t) + \mathbf{F}(\mathbf{x}(t)),\ t\ \in\ [T, \infty), \tag{39}$$

where $\mathbf{x}(t) = (W(t), R(t))^T$, Λ stands for the matrix:

$$\Lambda = \begin{pmatrix} -1 & 1 \\ 0 & -\frac{2\mu}{\lambda} \end{pmatrix}, \tag{40}$$

while $\mathbf{F}$ is defined by:

$$\mathbf{F} : A \subset \mathbb{R}^2 \to \mathbb{R}^2 : (\hat{W}, \hat{R}) \to \mathbf{F}(\hat{W}, \hat{R}) = 0,\ \ (\frac{1}{\lambda} - 1)\frac{\hat{W} - \lambda\hat{R}}{2(1 - \hat{W})}\hat{R}. \tag{41}$$

According to (34), we take:

$$A = \left\{ \mathbf{x} = (\hat{R}, \hat{W}) \quad | \quad |\mathbf{x}| \leq R < 1 \right\}, \tag{42}$$

where we employ: $|\mathbf{x}| = |x^1| + |x^2|$ as the norm of $I\!R^2$, [16]. On this A, it is easily seen that $\mathbf{F}$ is C^∞ actually analytic, and moreover it satisfies:

$$|\mathbf{F}(\mathbf{x})| \leq \left(M \frac{(1-\lambda)^2}{|\lambda|} \; |\mathbf{x}| \right) |\mathbf{x}| \leq N |\mathbf{x}|, \tag{43}$$

where

$$M = \max \;_{W \,\in\, A} \;\; |[2(1-\hat{W})]^{-1}| \;\; \text{and} \;\; N = \max \;_{x \,\in\, A} \left(M \frac{(1-\lambda)^2}{|\lambda|} |\mathbf{x}| \right).$$

Let now the IVP:

$$\frac{d\mathbf{x}(t)}{dt} \;=\; \Lambda \mathbf{x}(t) + \mathbf{F}(\mathbf{x}(t)), \;\; t \;\in\; [T, \infty), \tag{44}$$

$$\mathbf{x}(T) \;=\; \mathbf{x}_0, \;\;\; \mathbf{x}_0 \;\;\in\;\; A. \tag{45}$$

By the Picard-Lindelof's theorem [13], there exist unique solutions $\mathbf{x}(t)$ defined on $[T, \epsilon), \;\; \epsilon > 0$, and by the variation of constants formula [17] this solution is described by:

$$\mathbf{x}(t) = e^{(t-T)\Lambda} \mathbf{x}_0 + \int_T^t e^{(t-s)\Lambda} \mathbf{F}(\mathbf{x}(s)) ds, \;\;\; t \;\in\; [T, \epsilon). \tag{46}$$

Although this $\mathbf{x}(t)$ is defined only on $[T, \epsilon), \;\; \epsilon > 0$, as long as $|\mathbf{x}_0|$ is small enough and under some conditions upon the eigenvalue $\lambda_1 = -1, \;\; \lambda_2 = -\frac{2\mu}{\lambda}$ of Λ, it can be continued so that remains in $A \; \forall \; t \;\in\; [T, \infty)$. For that, let us suppose (λ, μ) are chosen so that $\lambda\mu > 0$. This restriction implies $\lambda_2 = -\frac{2\mu}{\lambda} < 0$ and thus both eigenvalues of Λ are negative. Standard estimates [13, 17] show that there exist $K > 0$ and $\rho > \max(\lambda_1, \lambda_2)$ such that:

$$|e^{(t-T)\Lambda}| \leq K e^{\rho(t-T)} \;\;\; \forall \;\; t \geq T. \tag{47}$$

As long as $\max(\lambda_1, \lambda_2) < 0$, we can always choose a ρ so that: $\max(\lambda_1, \lambda_2) < -|\rho| < 0$. For such ρ we obtain from (46) and (47):

$$|\mathbf{x}(t)| \leq K e^{-|\rho|(t-T)} |\mathbf{x}_0| + K \int_T^t e^{-|\rho|(t-s)} |\mathbf{F}(\hat{\mathbf{x}}(s))| ds. \tag{48}$$

Upon multiplying both sides by $e^{|\rho| t}$ we arrive at:

$$e^{|\rho| t} |\mathbf{x}(t)| \leq K e^{|\rho| T} |\mathbf{x}_0| + KN \int_T^t e^{|\rho| s} |\mathbf{x}(s)| ds, \tag{49}$$

where we made use of (43). By appealing to Gronwall inequality [18] we conclude that:

$$|\mathbf{x}(t)| \leq K |\mathbf{x}_0| e^{-(t-T)[|\rho| - KN]}, \;\; t > T, \tag{50}$$

and by shrinking the size of A if necessary, we can always make $|\rho| - KN > 0$ and thus the solution $\mathbf{x}(t)$ of (44,45) remains in A, $\forall \; t > T$.

This analysis shows that as long as $\lambda\mu > 0$, the solutions to the IVP (44,45) are dominated by the linear part and since both eigenvalues (λ_1, λ_2) are negative, they decay exponentially to zero as $t \to \infty$. To get more insights on their behavior we consider:

$$W(r) = \frac{c}{r} + \frac{c_1}{r^{1+\epsilon}}, \quad \epsilon > 0, \tag{51}$$

and returning to (30-33) we find:

$$\begin{aligned} W(r) &= \frac{c}{r} + \frac{c_1}{r^{\frac{2\mu}{\lambda}}}, & (52)\\ \rho(r) &= \frac{\rho_0}{r^{2+\frac{2\mu}{\lambda}}} + O\left(\frac{1}{r^3}\right), \ \rho_0 = -(\frac{2\mu}{\lambda} - 1)c_1, & (53)\\ \Phi(r) &= \Phi_0 - \frac{c}{2r} - \frac{c_1\lambda(1+2\mu-\lambda)}{4\mu}\frac{1}{r^{2\frac{\mu}{\lambda}}} + O(\frac{1}{r^2}). & (54) \end{aligned}$$

Always under the assumption $\lambda\mu > 0$, if $\lambda_2 < \lambda_1 = -1$ then $\frac{2\mu}{\lambda} = 1 + \epsilon, \ \epsilon > 0$ and thus:

$$\begin{aligned} W(r) &= \frac{c}{r} + \frac{c_1}{r^{1+\epsilon}}, & (55)\\ \rho(r) &= -\frac{\left(\frac{2\mu}{\lambda} - 1\right) c_1}{r^{2+\frac{2\mu}{\lambda}}} = -\frac{\epsilon c_1}{r^{3+\epsilon}}, \ \epsilon > 0, & (56)\\ \Phi(r) &= \Phi_0 - \frac{c}{2r} - \frac{c_1\lambda(1+2\mu-\lambda)}{4\mu}\frac{1}{r^{1+\epsilon}}, \ \epsilon > 0. & (57) \end{aligned}$$

If $\lambda_1 < \lambda_2 < 0$ then $\frac{2\mu}{\lambda} = 1 - \epsilon, \ \epsilon > 0$ and the solutions exhibit slower decay rates:

$$\begin{aligned} W(r) &= \frac{c}{r} + \frac{c_1}{r^{1-\epsilon}}, \ \epsilon > 0, & (58)\\ \rho(r) &= \frac{\rho_0}{r^{2+\frac{2\mu}{\lambda}}} = \frac{\epsilon c_1}{r^{3-\epsilon}}, \ \epsilon > 0, & (59)\\ \Phi &= \Phi_0 - \frac{c}{2r} - \frac{c_1(1+2\mu-\lambda)}{4\mu}\frac{1}{r^{1-\epsilon}}, \ \epsilon > 0. & (60) \end{aligned}$$

It is interesting to note that for the particular case where $1 - \lambda + 2\mu = 0$, we obtain $\lambda_2 = -\frac{2\mu}{\lambda} = -1 + \frac{1}{\lambda}$ and thus if $\lambda > 1$ then $\lambda_1 < \lambda_2 < 0$, which implies $\hat{k}\rho c^2 = O(r^{-(2+\epsilon)})$, while for $\lambda < 0$ $\lambda_2 < \lambda_1$, and thus $\hat{k}\rho c^2 = O(r^{-(3+\epsilon)})$. This behavior is in agreement with the exact solution described by (23,24).

There is an important difference between the asymptotic behavior of solutions described by (55-57) and those described by (58-60). The first family has finite ADM mass M_{ADM} while for the second family this mass is actually divergent. In order to see that, we notice that the spatial metric ${}^{(3)}\gamma$ can be written in the form:

$${}^{(3)}\gamma = \frac{dr^2}{1 - W(r)} + r^2 d\Omega^2, \ r \ \in \ (R_0, \infty), \tag{61}$$

and by employing conformal coordinates takes the form:

$${}^{(3)}\gamma = \hat{\Omega}^2(R)[dR^2 + R^2 d\Omega^2] = \hat{\Omega}^2(x)[dx^2 + dy^2 + dz^2], \tag{62}$$

where

$$\hat{\Omega}^2 = \left(\frac{dr(R)}{dR}\right)^2 \frac{1}{1 - W(r)}. \tag{63}$$

In order to evaluate the M_{ADM}, we employ the representation [19]:

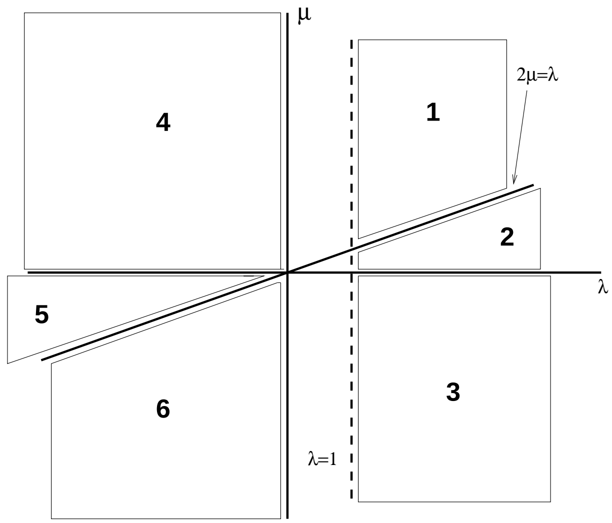

FIG. 6: Sketch of the parameter space (λ, μ). The regions labeled by $(3,4)$ do not generate solutions that decay to zero asymptotically. Regions labeled $(1,6)$ generate solutions decaying to zero at infinity but the decay is slow. Finally regions $(2,5)$ generate solutions that decay sufficiently fast so that they have finite ADM mass.

$$\begin{aligned} M_{ADM} &= \frac{1}{16\pi}\int_\Sigma [{}^3R(\gamma) + \frac{1}{4}\gamma^{mn}\gamma^{ab}\gamma^{cd}(2\gamma_{mn,d}\gamma_{ac,b} - 2\gamma_{ma,d}\gamma_{nc,b} \\ &\quad + \gamma_{dm,b}\gamma_{nc,a} - \gamma_{cd,a}\gamma_{mn,b})]\sqrt{\gamma}d^3x, \end{aligned} \tag{64}$$

where Σ stands for any asymptotic end defined by restricting r so that: $r > R_0$.
By appealing to the Hamiltonian constraint ${}^{(3)}R(\gamma) = 2\hat{k}\rho c^2$ and (62), the right hand side of (64) yields:

$$M_{ADM} = \int_\Sigma \left[2\hat{k}\rho c^2 - \frac{1}{2\hat{\Omega}^6(R)}\left(\frac{d\hat{\Omega}^2}{dR}\right)^2\right]\sqrt{\gamma}d^3x. \tag{65}$$

However it can be easily seen that this integral converges for the solutions described by (55,56) and diverges for those described by (58,59) (for more details see also [9]).

V. DISCUSSION

The results of the present paper can be succinctly summarized by partitioning the (λ, μ) plane according to whether the eigenvalues (λ_1, λ_2) of the matrix Λ satisfy: $\lambda_2 < \lambda_1$ or $\lambda_1 < \lambda_2 < 0$ (see Fig. 6). The values of (λ, μ) required to generate asymptotically flat solutions in the sense that the M_{ADM} is finite is indicated. Our analysis shows that solutions of (12-15) subject to (20,21) if they are decaying as $r \to \infty$, then (λ, μ) should lie in the regions $(1,2)$ and $(5,6)$ of Fig. 6 and the decay rates are those described in (55-57) and (58-60). It is important however to stress a point. Although the numerical outputs show that there exist initial conditions so that the solutions are decaying as $r \to \infty$ and moreover are asymptotically flat whenever (λ, μ) are taken in regions $(2,5)$, we have not shown that for any (λ, μ), lying on regions (2) or (5) of Fig. 6, there exist initial conditions so that the solutions of (12-15) are reaching the asymptotic region. This for the moment is an open issue.

Our results establish the existence of reflectionally symmetric asymptotically flat wormholes having throat of arbitrary area. This conclusion is a consequence of the rescaling property of the solutions under rescaling of the throat area. As far as non reflectional wormholes are concerned, the graphs in Figs. 4-5 show that they do exist (notice for these figures $\lambda_2 < -1$). However they do not exist for all values of $\Lambda(0)$. The numerical outputs show that after some critical values of $\Lambda(0)$ the solutions become unbounded. This suggests that $A(0)$ and $\Lambda(0)$ may not be taken independently although the nature of any constraint of this sort is for the moment unknown [20].

Acknowledgments

It is our pleasure to acknowledge many stimulating discussion with the members of the relativity group at IFM-UMSNH, in particular J. Estevez-Delgado and Olivier Sarbach. This work was supported in part by grants: CIC-UMSNH 4.7, 4.9 and 4.23, SEP-PROMEP UMICH-CA-22, UMICH-PTC-210, COECyT Michoacán S08-02-28 and E9507, CONACyT 79601 and 79995.

VI. REFERENCES

[1] A. G. Riess *et al*, ApJ **116**, 1009 (1998); S. Perlmutter *et al*, Nature, **391** 51 (1998); A. G. Riess *et al*, ApJ **118**, 1009 (1999); S. Perlmutter *et al*, ApJ **517**, 565 (1999); A. G. Riess *et al*, ApJ **536**, 62 (2000); A. G. Riess *et al*, ApJ **560**, 49 (2001).

[2] C. B. Netterfield *et al*, Astrophys. J. **571**, 604 (2002).

[3] C. L. Bennett *al*, Astrophys. J. Suppl. **148**, 1,(2003). ArXiv: astro-ph/0302207.

[4] A. G. Riess *et al*, Astrophys. J. **607** 665 (2004). ArXiv: astro-ph/0402512.

[5] M.S. Morris and K. Thorne, Am. J. Phys. **56**, 395 (1998).

[6] S. Sushkov, Phys. Rev. D **71** , 043520 (2005).

[7] F. S. Lobo, Phys. Rev. D **71**, 084011 (2005).

[8] Although we are ignorant of the microphysics describing exotic matter and thus we cannot justify the choice for the EOS employed in the present work, our aim is to address the global existence of spherical wormholes away from the usual approach where one first specifies the wormhole metric and subsequently tailor the structure of exotic matter required to support it.

[9] N. Montelongo-García and T.Zannias, Constructing Spherical Traversable Wormholes: An Initial Value Approach, (submitted, 2008).

[10] N. Montelongo-García and T. Zannias, Phys. Rev. D **78**, 064003, (2008).

[11] Ought to be stressed that by utilizing eq. (8) one of the four variables can be expressed in terms of the other three. For instance: $\lambda\hat{k}\rho(l)c^2 = \hat{r}^2(l) - \frac{K^2(l)}{4} - \Lambda(l)K(l)$ and upon subsituting this expression into eq. (7) we find that it is identically satisfied by virtue of (4,5) and (6). Thus the system (4-8) is a system of three eqs for three unknowns. As such the initial condition for $\rho(0)$ cannot be chosen independently, a point that is clearly reflected in the initial conditions described in eqs. (10,20) and (21). Since we resort into grafical representations of the solutions, we shall consider (4-8) as a system of four eqs. for four variables. In this way the numerical plots exhibit the behavior of the geometrical as well as the matter variables.

[12] In a cosmological setting, a phantom configurations is restricted by the requirement that observeres comoving with the cosmological expansion measure $\rho c^2 > 0$. The choice $(\rho(0) < 0, \lambda < 0)$ is consistent with the wormhole initial conditions and thus we shall analyze this case as well. It may be worth recalling that massless K-essence belongs to this latter family of exotic matter.

[13] P. Hartman: Ordinary differential equations, Wiley (1964).

[14] This property of solutions is a generic property of the system (see for instance discussion in [10]).

[15] J. A. González, F. S. Guzmán, N. Montelongo-Garcia and T. Zannias, An exact two parameter family of spherical wormholes, (submitted, 2008).

[16] The norm $|\ ,\ |$ employed in the text is related to the standard Euclidean norm $||\ ,\ ||$ of $I\!R^2$ via: $||\mathbf{x}|| \leq |\mathbf{x}| \leq \sqrt{2}||\mathbf{x}||$ i.e. $|\ ,\ |$ and $||\ ,\ ||$ are equivalent norms.

[17] See for instance: Coddington E. A., Levinson N., Theory of ord. dif. eqs., TMH edition, McGraw-Hill, (1972), L.Perko, Differential Equations and Dynamical Systems, Springer-Verlag (1991).

[18] We recall that this inequality states that if $K \geq 0$ and (f, g) are non negative functions in $C[a, b]$ satisfying: $f(t) \leq K + \int_\alpha^t f(s)g(s)ds$, $t \in [a, b]$ then $f(t) \leq Ke^{\int_\alpha^t g(s)ds}$ (see for instance [13, 17]).

[19] N. O. Murchadha, J. Math. Phys. **27**, 2111, (1986).

[20] It is worth noting that if we set $V(l) = e^{\Phi(l)}$ then by appealing to eqs (4-8) we obtain: $\nabla^2 V = \frac{\hat{k}V}{2}(\rho c^2 - \tau + 2P)$ from where it follows that the Komar mass M_K of an asymptotically flat end satisfies: $M_K \approx \frac{V(0)A(0)\Lambda(0)}{2} + \frac{\hat{k}}{2}\int V[\rho c^2 - \tau + 2P]\sqrt{\gamma}d^3x$ suggesting that the parameter $\Lambda(0)$ affects the Komar mass of the asymptotic end. The issue of the relation between the ADM and Komar masses of an end is a delicate one and we shall not address it in this work. We only add that any relation between these masses may be relevant in understanding some of the issues raised in this work.